

EXCITATION OF MOLECULAR MATERIAL NEAR THE YOUNG STELLAR OBJECT LKH α 234 IN NGC 7129

PATRICK W. MORRIS¹, ALBERTO NORIEGA-CRESPO, FRANCINE R. MARLEAU, HARRY I. TEPLITZ
Spitzer Science Center, IPAC, Caltech, MS 220-6, Pasadena, CA 91125

KEVEN I. UCHIDA

Center for Radiophysics and Space Research, Cornell University, Ithaca, NY 14853-6801

AND

LEE ARMUS

Spitzer Science Center, IPAC, Caltech, MS 220-6, Pasadena, CA 91125

Accepted for publication in the Spitzer edition of the Astrophysical Journal Supplement Series

ABSTRACT

With the *Spitzer*-IRS² we have obtained the first mid-IR spectroscopy of NGC 7129, in the unusually strong outflow and in a ridge of H₂ emission near the Herbig Be star LkH α 234. The UV radiation field strength is estimated from PAH band intensities in the H₂ ridge, and found to be comparable to that of NGC 7023. From the rotational H₂ emission lines we have deduced aperture average excitation temperatures and column densities in the two regions, finding the H₂ ridge values to be consistent with pumping by UV fluorescence, but also comparable to warm-gas regions of Cep A that form H₂ in non-dissociative C-shocks. The H₂ emission in the outflow is consistent with formation by collisional excitation in J-shocks, with shock velocities of 10 – 30 km sec⁻¹. A photodissociating component may be present in the outflow, by similarity of S(0) line intensities in both regions. There is no indication of warm dust in the outflow. We also present the first 16 μ m imaging of a Galactic nebula using the unique imaging capabilities of the IRS, and combine with ground-based 2.12 μ m (H₂ 1 – 0 S(1)) imaging. Candidate pre-main sequence objects are clearly evident in these data. We also find extended emission not previously observed around the young B star BD +65°1638, \sim 22'' across, showing that the region is not free of material as otherwise inferred by recent high angular resolution mapping at submillimeter wavelengths. The presence of this material complicates interpretation of the surrounding CO cavity and origin(s) of the photodissociated region, and further spectroscopic observations are needed to characterize its nature.

Subject headings: infrared: ISM — ISM: jets and outflows — ISM: individual (NGC 7129) — reflection nebulae — stars: formation — stars: pre-main sequence — infrared: stars

1. INTRODUCTION

NGC 7129 in Cepheus is a prototype young star-forming region and well-known reflection nebula, dominated by two young intermediate-mass ($M \simeq 3 - 10M_{\odot}$) B stars, and the unusual Herbig Be star LkH α 234. The winds from the early-type B stars, BD +65°1637 and BD +65°1638 (B2-B4; Strom et al. 1972; Hillenbrand et al. 1992), but chiefly from the latter which is probably the older (Racine 1968), have created a cavity of CO emission near the center of the nebula, and dense ridges of molecular material to the east, south, and west (Mitchell & Matthews 1994; Fuente et al. 1998; Eislöffel 2000; Miskolczi et al. 2001). Atomic and molecular lines observed in an 80'' beam with the Infrared Space Observatory Long Wavelength Spectrometer (LWS) indicate that the emission originates from photodominated excitations, possibly in high density or clumpy environments as well (Lorenzetti et al. 1999; Giannini et al.

1999). LkH α 234 is estimated to be the youngest of these dominant stellar sources (Hillenbrand et al. 1992), probably formed in response to the compression of material on the northern edge (Mitchell & Matthews), and is in a center of star forming activity that includes several pre-main sequence (PMS) objects, observed at millimeter wavelengths with high angular resolution (Fuente et al. 2001). A low velocity (\sim 10 km sec⁻¹) outflow extends over \sim 12' from LkH α 234 (Edwards & Snell 1983), possibly as far as \sim 22' or some 8 pc as projected onto the sky (McGroarty, Ray, & Bally 2004) at a distance of 1.25 kpc to NGC 7129 (Shevchenko & Yakubov 1989), and an optical jet extends into the cavity (Ray et al. 1990). The outflow and jet likely originate from a PMS object offset from LkH α 234, as suggested by Cabrit et al. (1997) and then localized by Fuente et al. (2001) to a source \sim 3''.5 to the NW.

In this paper we present the first mid-infrared spectra of two regions, one in the outflow, and one in the ridge of H₂ emission near LkH α 234, with the aim of exploring the excitation conditions in the environment surrounding this young star in its early stages of evolution. We estimate the intensity of the UV radiation field from the strengths of the polyaromatic hydrocarbon (PAH) band strengths, and determine the excitation mechanism responsible for H₂ line emission. Imaging the nebula at

¹ NASA *Herschel* Science Center, IPAC, Caltech, MS 220-6, Pasadena, CA 91125

²The *Spitzer* Space Telescope is operated by the Jet Propulsion Laboratory, and Caltech Institute of Technology under NASA contract 1407. Support for this work was provided by NASA through an award issued by JPL/Caltech. The IRS was a collaborative venture between Cornell University and Ball Aerospace Corporation funded by NASA through the Jet Propulsion Laboratory and the Ames Research Center.

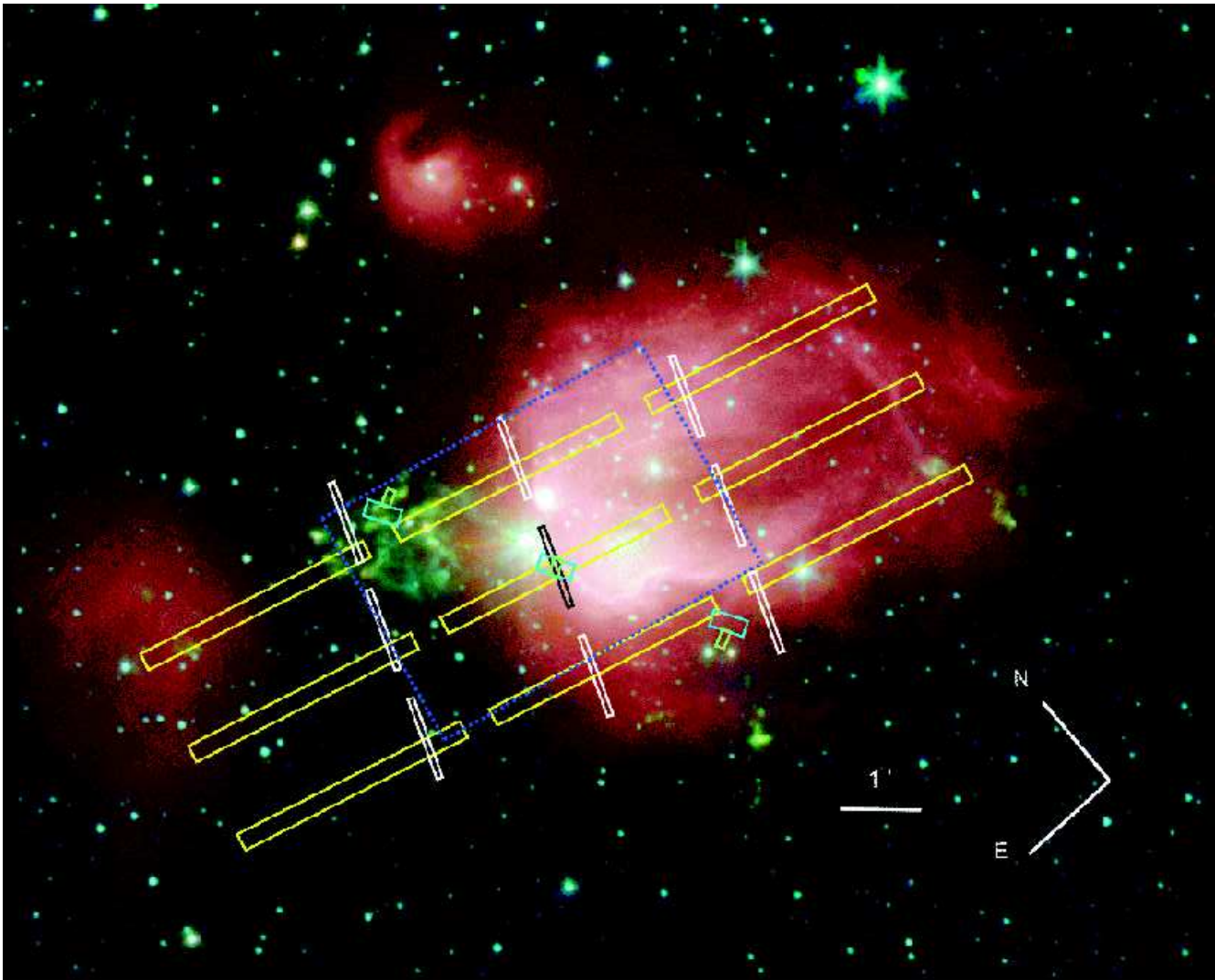


FIG. 1.— Position of the IRS spectral slits on NGC 7129, 11 November 2003. The slits are Short Low (white or black), Long Low (yellow), Short High (green), and Long High (blue). The $14' \times 12'$ image is an IRAC mosaic with the 3.6 (blue), 4.5 (green), 5.8 (orange), and $8.0 \mu\text{m}$ (red) filters (see Gutermuth et al. 2004). The blue dotted line indicates where IRS $16\mu\text{m}$ and ground-based $2.12 \mu\text{m}$ mapping have been obtained (Fig. 2).

$2.12 \mu\text{m}$ ($\text{H}_2 1 - 0 \text{S}(1)$) and $16 \mu\text{m}$ (continuum plus $\text{H}_2 0 - 0 \text{S}(1)$) gives us a larger scale view on the spatial distribution of molecular gas.

2. SPECTROSCOPY AND IMAGING

2.1. IRS Spectroscopy

NGC 7129 was observed on 11 November 2003 with the Infrared Spectrograph (IRS, described by Houck et al. 2004, this volume) onboard the *Spitzer* Space Telescope (Werner et al. 2004a, this volume). A spectral map was performed with the slits centered on the H_2 ridge in the photodissociated region (PDR), at $21^{\text{h}}43^{\text{m}}04.82^{\text{s}} + 66^{\circ}06'27''.7$ (all positions J2000.0), $29''.5$ arcsec SW of LkH α 234. The map also includes a position in the strong molecular outflow, $21^{\text{h}}43^{\text{m}}19.8^{\text{s}} + 66^{\circ}07'50''.7$. Our analyses are concentrated on these two positions, nearest to LkH α 234, and where the fullest wavelength coverage among the separate slits is most spatially confined (as described further below). All slit positions on the nebula

are shown in Fig. 1, using the Early Release Observation² of the nebula, obtained with the Infrared Array Camera (IRAC; Fazio et al. 2004, this issue) at 3.6, 4.5, 5.8, and $8.0 \mu\text{m}$.

Spectroscopy was obtained with each of the IRS modules, using total exposure times of 48 seconds with the Short Low module (SL, spanning $5.3 - 14.5 \mu\text{m}$ at spectral resolution $R = \lambda/\Delta\lambda \simeq 80 - 120$), 90 seconds with Short High (SH, $10 - 19.7 \mu\text{m}$, $R \simeq 700$), and 120 seconds with Long High (LH, $18.8 - 37 \mu\text{m}$, $R \simeq 700$) at each slit position. Long Low (LL, $14 - 38 \mu\text{m}$, $R \simeq 80 - 120$) data were also obtained, providing an internal check of the consistency with overlapping SH and LH data. The relative spectrophotometry is consistent to within 10% over the same sky area, and the LL data contain no new spectral information, rather degraded at the lower spec-

² <http://www.spitzer.caltech.edu/Media/releases/ssc2004-02/ssc2004-02a.shtml>. See also Gutermuth et al. (2004) and Muzerolle et al. (2004).

tral resolution; therefore we present only the SH and LH data here. The raw data have been processed in the SSC S9.1 pipeline to Basic Calibrated Data (BCD) products, and then extracted to 1-D spectra using the offline version of the post-BCD pipeline. A region of $3''.6 \times 13''.5$ on the central map position was extracted from the SL data at $10 \mu\text{m}$. The full SH and LH slits were extracted and then scaled to the SL spectrum. Two or three individual spectra over each wavelength range were obtained at each extracted position, and these were flux-calibrated, coadded, and sigma-clipped to produce a single spectrum of the H $_2$ ridge spanning $5.3 - 37 \mu\text{m}$, and an outflow spectrum over $7.5 - 37 \mu\text{m}$. Absolute fluxes are estimated to be uncertain by $\sim 20\%$ overall (Decin et al. 2004).

2.2. Ground-Based 2.12 μm and IRS 16 μm Imaging

The H $_2$ 1 – 0 S(1) 2.12 μm data were obtained on 2003 November 10 – 12 with the 3.6m telescope at the Canada-France-Hawaii Telescope (CFHT) using the CFHTIR camera. The camera provides a $3''.6 \times 3''.6$ field of view and a scale of $0''.211 \text{ pixel}^{-1}$. The data were dark subtracted, flatfielded, and sky corrected in IRAF, using the special near-IR data reduction package DIMSUM³. The H $_2$ image has a total integration time of 18 minutes, and been resampled to match the pixel scale of the 16 μm IRS image.

Mid-IR imaging of NGC 7129 was obtained with the IRS 16 μm camera on 10 October 2003 and 29 November 2003. Individual data frames were reduced in the S9.1 SSC pipeline to BCD products, and then registered based on reconstructed pointing, which is accurate to $\sim 0.7''$ ($1-\sigma$ radial). The 16 μm and 2.12 μm mosaic is shown in Fig. 2. Several pixels are saturated at 16 μm by the three identified objects. In this field, Muzerolle et al. (2004, this issue) have proposed several PMS objects on the basis of the colors extracted from IRAC and MIPS, three of which are clearly evident by their 16 μm emission in Fig. 2. White arrows identify candidate Class 0/I objects, the yellow arrow corresponds to a Class II object. At least one other PMS object in this field is proposed by Muzerolle et al., but is not evident by a 16 μm thermal excess.

Fig. 2 also shows an arc of 16 μm emission in the vicinity of BD +65 $^\circ$ 1638, almost concentric with the eastern H $_2$ ridge. This structure is not discerned in IRAC or MIPS imaging (cf. Gutermuth et al. 2004 and Muzerolle et al. 2004), possibly as a consequence of the temperature and surface brightness of the material. At moderate angular resolution ($1'$), Matthews et al. (2003) identify a dense concentration of neutral hydrogen (21 cm) coincident with BD +65 $^\circ$ 1638, as well as an extensive region of photodissociated H $_2$ accompanied by a small H II region around this star. Miskolczi et al. (2001) have proposed that the cavity of molecular material around BD +65 $^\circ$ 1638 has been created by photodissociation of H $_2$ into neutral hydrogen, and that the gas and radiation pressure from within the cavity are responsible for sweeping material into a shell that appears as the H $_2$ ridge. The presence of this concentrated structure (acknowledging some saturation of an area of radius $\sim 2''.5$

centered on BD +65 $^\circ$ 1638) clearly shows that material, either molecular gas or dust, is not entirely evacuated from this region. Further spectroscopy is needed determine its properties.

TABLE 1
ROTATIONAL H $_2$ 0 – 0 OBSERVED FLUXES, COLUMN DENSITIES, AND EXCITATION TEMPERATURES^a.

Line [μm]	PDR			Outflow		
	Flux	$\ln(N/g)$	E_{up}/k	Flux	$\ln(N/g)$	E_{up}/k
S(6) 6.11	61.0 (1.3) ^b
S(5) 6.91	23.0 (1.7) ^c	38.55	4415
S(4) 8.02	41.0 (2.5) ^b
S(3) 9.66	8.75 (0.77)	40.01	2333
S(2) 12.28	1.20 (0.03)	40.84	1682	0.54 (0.02)	40.04	1682
S(1) 17.03	1.70 (0.04)	42.41	844	0.54 (0.02)	41.27	844
S(0) 28.22	0.37 (0.02)	45.60	510	0.33 (0.01)	45.49	510
		N_{tot}	T_{ex}		N_{tot}	T_{ex}
		1.17 (0.04)	658 (9)		13.4 (0.7)	248 (12)

^aFluxes in units of $10^{-11} \text{ W cm}^{-2} \text{ sr}^{-1}$, uncertainties are in parentheses. Excitation temperature T_{ex} is in K, and total column density density N_{tot} is in 10^{19} cm^{-2} .

^bSeverely blended with neighboring PAH band.

^cBlended with neighboring PAH band.

3. SPECTROSCOPIC RESULTS

The IRS spectra of the PDR/H $_2$ ridge and outflow are presented in Fig. 3, as labeled. The spectra are not offset from each other. Sky background levels indicated by the triangles at 10, 24, and 30 μm are estimated from a *Spitzer*-centric, COBE/DIRBE-based⁴ model of the thermal emission by zodiacal and ISM dust in the line of sight to NGC 7129, on its date of observation. At these levels, we surmise that the outflow contains negligible amounts of warm dust.

The PDR spectrum exhibits the usual set of PAH bands, at peak positions of 6.22, 7.63, 8.63, 11.22, 12.75, and 16.46 μm , dominated by the 7.63 and 11.22 μm bands. Secondary peaks that may be associated with PAH emission are present at 11.00, 11.99, 13.55, 14.24, and possibly 17.37 μm . These features are not previously identified, to our knowledge, and Werner et al. (2004b, this volume) identify other new subsidiary bands in IRS spectra of the NGC 7023 reflection nebula, including the 17.4 μm feature.

The strength of the PAH band emission allows us to estimate the intensity of the UV radiation field in the vicinity of LkH α 234. Using a two-component blackbody with temperatures 75 K and 320 K and unity emissivity to approximate the thermal continuum, we measure strengths of the 6.22, 7.63, 11.22, and 12.75 μm bands in the range of $6.0 - 30 \times 10^{-5} \text{ W m}^{-1} \text{ sr}^{-1}$. The observational trend of PAH band intensities plotted against UV radiation field density by Boulanger et al. (1998) for a set of PDRs implies a field strength of 800 to 900 times the solar value. This is close to the value of NGC 7023, which is measured by Boulanger et al. from a region of maximum emission in the PDR, in proximity to the PMS Herbig B2-B3 star HD 200775 which is similar to our PDR location near BD+65 $^\circ$ 1638, without consideration in either case for shielding by circumstellar material. And like NGC 7023, the PAH bands are lower in

³ The Deep Infrared Mosaicing Software package of IRAF scripts, developed by P. Eisenhardt, M. Dickinson, A. Stanford, and J. Ward, available at ftp://iraf.noao.edu/contrib/dimsumV2

⁴ Available in the SPOT observations planning tool.

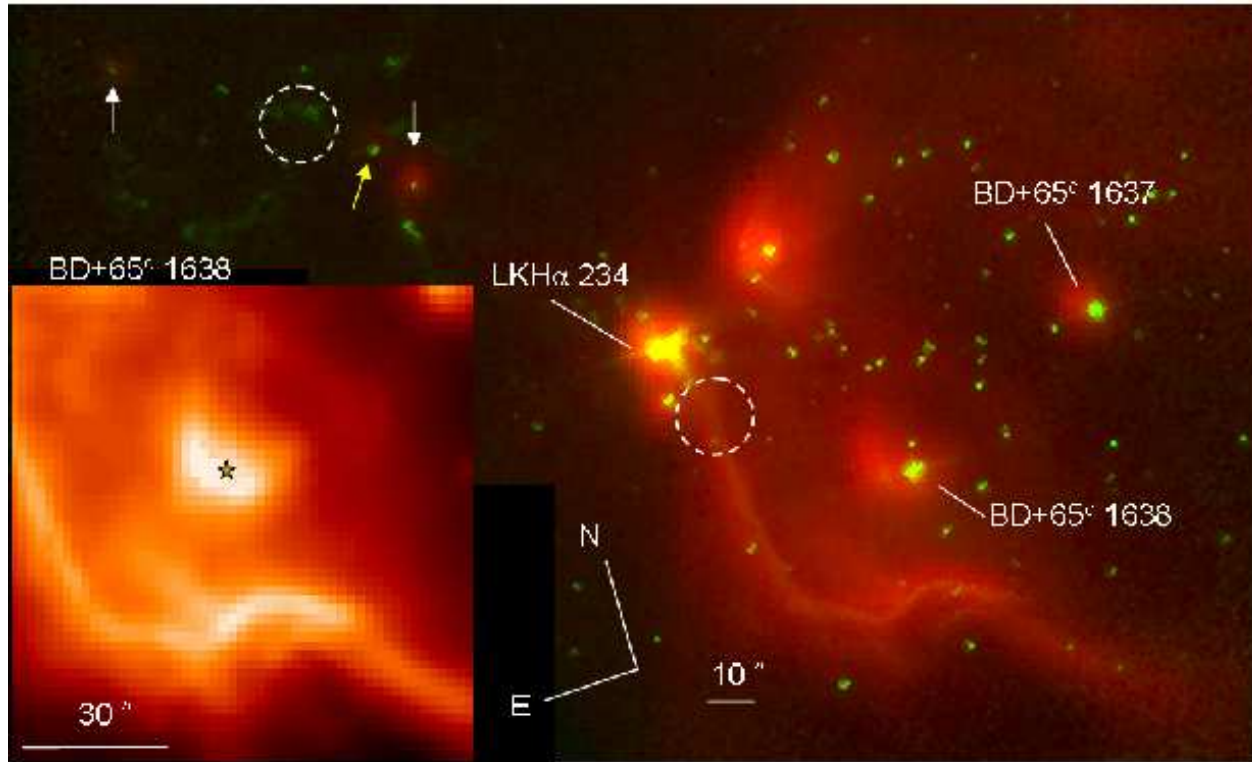


FIG. 2.— IRS 16 μm (red) and CFHT 2.12 μm (green) mosaic of NGC 7129. The bandpass of the 16 μm camera covers 13.3 – 18.7 μm . Individual frames cover $54'' \times 82''$ with a pixel scale of $1''.8$. A mosaic of 25 positions, with 140 seconds of integration time per pixel on the sky, was obtained to cover an area of approximately $4'.3 \times 2'.5$. Regions of spectroscopic analysis are indicated by the circles with dashed lines. Candidate PMS objects are indicated by the yellow and white arrows. A region of $\sim 80'' \times 85''$ around BD +65°1638 at 16 μm is shown in the inset, to bring out details of structured emission around the star, and the region of relative maximum surface brightness in the H₂ ridge.

intensity at this UV field strength than given by a simple power law extrapolation from PDRs with lower field strengths. This could be due to a lower abundance of small dust grains in high radiation fields, as suggested by Boulanger et al.

The PDR and outflow spectra both exhibit pure rotational lines of H₂, arising from optically thin quadrupole transitions that are readily thermalized at moderate volume densities. This allows us to estimate H₂ column densities and excitation temperatures under the assumption of LTE (e.g., Gredel 1994), in order to gain insight into the excitation conditions of the line forming regions. We follow excitation diagram methods developed by Burton (1992) and Gredel (1994), and applied to comparable environments (as in, e.g., Cepheus E by Moro-Martin et al. 2001). The column density for transition j is $N_j = 4\pi F_j / \Omega E_j g_j A_j$, where E_j is the energy of the upper level, g_j is the statistical weight of ortho- and para-transitions, and A_j is the transition probability. The line column density is related to the total column density and excitation temperature T_{ex} by $\ln(N_j/g_j) = \ln(N_{\text{tot}}/Q) - E_j/(kT_{\text{ex}})$, and may be solved for with a Boltzmann excitation diagram. The partition function Q was determined with an ortho-para ratio of 3 under the assumption of thermal equilibrium (Moro-Martin et al. 2001). For the observed line fluxes per unit solid angle F_j/Ω , we have extracted over regions of 40 arcsec² and 62 arcsec² in the 5.3 – 14 μm and 14 – 35 μm ranges, respectively. In these areas we must

view our measurements as spatially integrated. The computed values for $\ln(N_j/g_j)$, E_{up}/K along with the final estimates of the total H₂ column density and excitation temperature for the PDR and outflow are listed in Table 1. The observed line fluxes per unit solid angle F_j/Ω , 1- σ measurement uncertainties, and computed values of $\ln(N_j/g_j)$, E_{up}/k along with final estimates of the total H₂ column density and excitation temperature for the PDR and outflow are listed in Table 1. The lines were measured with the line-fitting utilities in the ISAP⁵, which allows multiple fits of Lorentzian and Gaussian profiles for deblending, suited to the PAH features (e.g., Boulanger et al. 1998) and the unresolved H₂ lines. This permits the H₂ S(4) and S(5) fluxes to be separated from the 7.6 and 8.6 μm PAH bands. The PDR line intensities are corrected for reddening using the Draine & Lee (1984) extinction law, and $A_V = 2.6$ mag estimated by Hamann & Persson (1992) towards LkH α 234. The extinction across the nebula probably varies widely, and the ISM component is likely to be much lower along the line of sight to our H₂ ridge observation, but the differences to the S(0) – S(2) lines will be small (< 5%), and measurement uncertainties of the S(3) – S(5) lines arise predominantly from the blending with the PAH features and the flux calibration. The S(6)/S(5) or S(4)/S(5) line ratios could be also affected by an ortho-para ratio differ-

⁵ ISO Spectral Analysis Package:
<http://www.ipac.caltech.edu/iso/isap/isap.html>

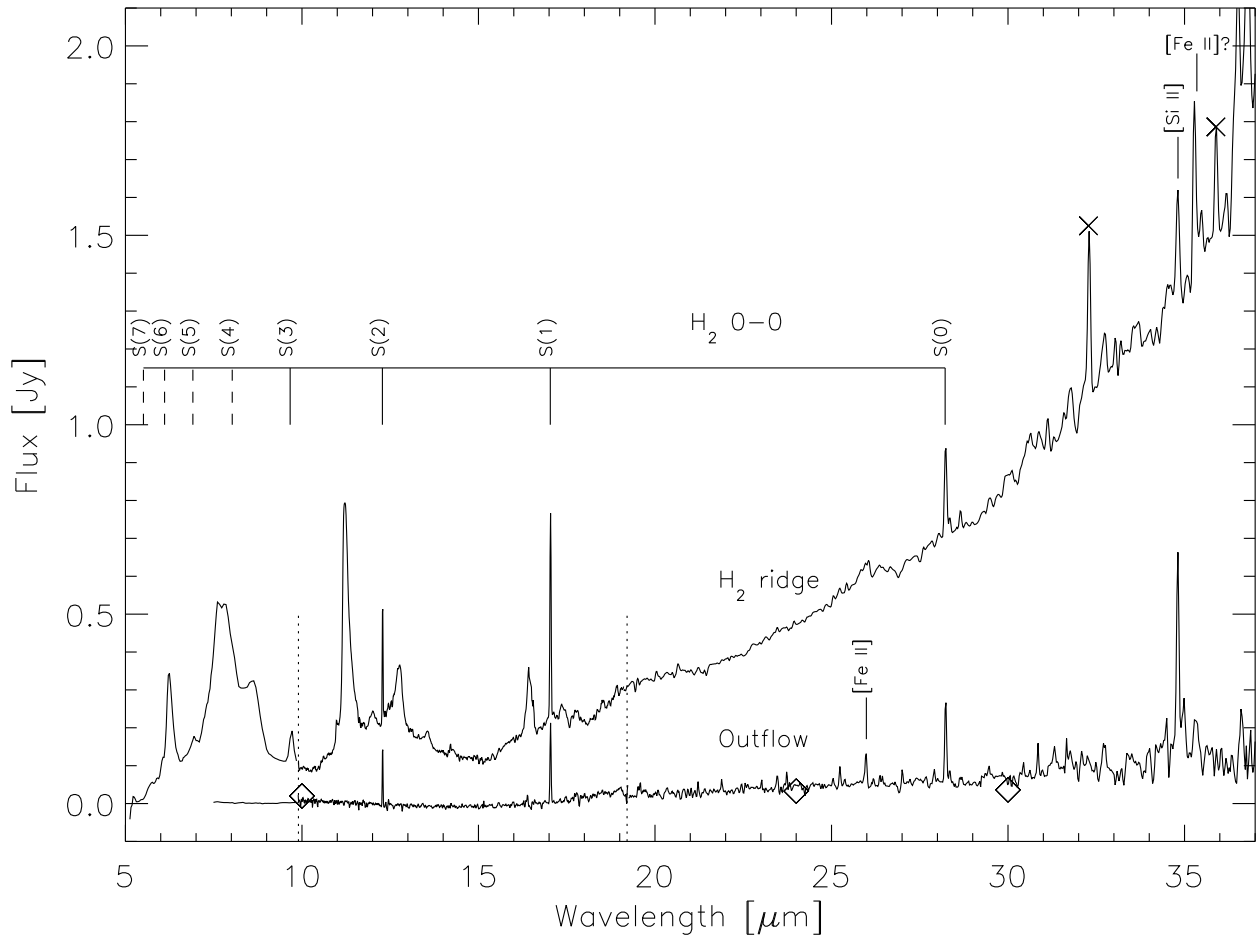


FIG. 3.— IRS spectra of the outflow and PDR near LkH α 234, as indicated. Data are on their natural flux scales, without offsetting. Diamonds represent emission levels of the sky (ISM and zodiacal light) background. The atomic nebular and H $_2$ rotational are identified, where dashed lines indicate where H $_2$ lines in the SL range are severely blended with surrounding PAH emission. The dotted lines show where the SL, SH, and LH data have been joined. Cosmic ray artifacts are indicated by "x".

ent than the canonical (thermal equilibrium) value of 3, as in the presence of shocks (Wilgenbus et al. 2000), or by the superposition of multiple layers along the line of sight with different physical conditions. From this standpoint we must view our spatially-limited measurements as mean indicators of the physical conditions in both the PDR and outflow.

The factor ~ 2.5 in T_{ex} between the PDR and the outflow seems quite reasonable, for line emission in the outflow arising from collisional (dissociative J-shock) excitation. We favor the J-shock mechanism over C-shocks in the outflow, based on the S(0) line intensity and strong [Si II] 34.815 μm emission. In the outflow the [Si II] and [Fe II] line fluxes are $1.06 (\pm 0.15) \times 10^{-20}$ and $2.36 (\pm 0.38) \times 10^{-21} \text{ W cm}^{-2}$, respectively. In the PDR, the [Si II] line flux is $7.92 (\pm 0.13) \times 10^{-21} \text{ W cm}^{-2}$. Interestingly, the measured line intensities of the S(0) line in the PDR and outflow are quite similar, which might be explained by a photodissociating component in the outflow. As for velocities, Edwards & Snell (1983) measured a maximum CO expansion of 10 km sec $^{-1}$, associated with the outflow. In J-shock models (Hollanbach & McKee 1989) for a faster jet-related component, H $_2$ lines

are not a good diagnostics of shock velocities, as their intensities are almost flat as function of velocity at the densities we expect ($\sim 10^5 \text{ cm}^{-3}$). But we know from the absence of [Ne II] and presence of H $_2$ that the velocity must be less than 50 km sec $^{-1}$. At the densities and low T_{ex} we measure, we estimate J-shock velocities in the range of 10 – 30 km sec $^{-1}$.

The H $_2$ spectrum (and thus the T_{ex} we infer) for the H $_2$ ridge can be explained by the standard Draine & Bertoldi (1996) models for a stationary PDR, and are similar to conditions in the S 140 PDR (Timmermann et al. 1996). This does not rule out contribution from non-radiative processes that are reasonable in this environment, where either or both of BD +65 $^{\circ}$ 1638 and BD +65 $^{\circ}$ 1637 are sweeping material outwards by mechanical wind momentum, to form some H $_2$ by collisional excitation. Indeed far infrared spectroscopic observations of the LKH α 234 region with multiple pointings using the ISO-LWS (Lorenzetti et al. 1999) already indicate that the PDR is the dominant component for the H $_2$ fluorescent emission, but the presence of C-shocked material cannot be ruled out. Our observations lack the spatial information with additional pointings to make a

comparison with a more complex, clumped PDR model (e.g., Burton et al. 1990) as done by Lorenzetti et al. (1999; see their Fig. 6). It is anyway useful to note that collisional excitation, if present in a clumped environment, cannot be done in cooling zones behind dissociative J-shocks (cf. Hollenbach & McKee 1989), where T_{ex} is lower than 300 – 400 K at our densities, but more likely in C-shocks with pre-shock H_2 volume density, magnetic field, ionization fraction, and shock speed conditions found, for example, in GGD37 in Cepheus A West (Wright et al. 1996). This region is also a site of intermediate mass star formation with a massive outflow, and bow-shock like clumps and filaments of H_2 emission (Hartigan et al. 1996), exhibiting very comparable H_2 rotational line fluxes (and $T_{\text{ex}} \simeq 700$ K). Aperture average column densities are one order of magnitude higher than in the NGC 7129 H_2 ridge, which gives us a correspondingly lower H_2 mass of $\sim 10^{-3} M_{\odot}$.

4. SUMMARY AND CONCLUSIONS

With the IRS we have obtained the first mid-IR spectroscopy of regions around LkH α 234, in the recognizable outflow and in a nearby ridge of H_2 emission. The measured intensities of the PAH bands in the H_2 ridge allowed us to infer the strength of the UV radiation field, which is comparable to that estimated by Boulanger et al. (1998) in NGC 7023. The rotational H_2 emission line ratios infer an (LTE) aperture average excitation temperature of 657 K and column density of $1.2 \times 10^{19} \text{ cm}^{-2}$, quite similar to the warm- H_2 regions of Cep A that are well matched by formation in non-dissociative C-shocks.

The cooler H_2 emission in the outflow is consistent with formation by collisional excitation in J-shocks, with velocities of 10 – 30 km sec $^{-1}$. A photodissociating component is suggested by similarity of S(0) line intensities in the outflow and PDR/ H_2 ridge. There is no significant contribution of thermal emission from warm dust in the outflow.

The origin of the PDR cannot be localized with certainty from the IRS observations presented here. Lorenzetti et al. (1999) presented ISO-LWS observations of [C II] 158 μm , [O I] 63 μm , and [O I] 146 μm emission whose spatial morphology and derived densities and UV field strength across the nebula favor BD+65 $^{\circ}$ 1637, arguing that this is consistent with observations by Fuente et al. (1998) of a ^{13}CO cavity created by the young star. Miskolczi et al. (2001) have subsequently shown with ^{12}CO and ^{13}CO maps that the cavity is instead centered on the older star BD+65 $^{\circ}$ 1638, which Matthews et al. (2003) recently find in 21 cm maps to be surrounded by an extensive photodissociated H_2 and a small H II region. On the other hand, our detection of warm material at 16 μm around BD+65 $^{\circ}$ 1638 clearly shows that this region is not free of material, and though BD+65 $^{\circ}$ 1638 is not an embedded object, further spectroscopic observations are needed to ascertain its nature.

We thank Louise Edwards and the CFHT staff for their help with the CFHTIR observations. We also thank an anonymous referee for helpful comments on the manuscript.

REFERENCES

- Boulanger, F., Abregel, A., Bernard, J. P., et al. 1998, in Star Formation with the Infrared Space Observatory, ASP Conf. Ser. 132, ed. J. L. Yun & R. Liseau (San Francisco: ASP), 15
- Boulanger, F., Boissel, P., Cesarsky, D., & Ryter, C. 1998 A&A, 339, 194
- Burton, M. G. 1992, AuJPh, 45, 463
- Burton, M. G., Hollenbach, D. J. & Tielens, A. G. G. 1990, ApJ, 365, 620
- Cabrit, S., Lagage, P.-O., McCaughrean, M., & Olofsson, G. 1997 A&A, 321, 523
- Decin, L., Morris, P. W., Appleton, P. N., Charmandaris, V., & Armus, L. 2004, ApJS, this volume.
- Draine, B. T., & Bertoldi, F. 1996, ApJ, 468, 269
- Edwards, S., & Snell, R. L. 1983, ApJ, 270, 605
- Eisloffel, J. 2000, A&A, 354, 236
- Fazio, G., et al. 2004, ApJS, this volume
- Fuente, A., Martin-Pintado, J., Bachiller, R., Neri, R., & Palla, F. 1998, A&A, 334, 253
- Fuente, A., Neri, R., Martin-Pintado, J., et al. 2001, A&A, 366, 873
- Giannini, T., Lorenzetti, D., Tommasi, E., et al. 1999, A&A, 346, 617.
- Gredel, R. 1994, A&A, 292, 580
- Gutermuth, R., et al. 2004, ApJS, this volume.
- Hartigan, P., Carpenter, J. M., Dougados, C., & Strutskie, M. F. 1996, AJ, 111, 2470
- Hillenbrand, L. A., Strom, S. E., Vrba, F. J., & Keene, J. 1992 ApJ, 397, 613
- Hollenbach, D., & McKee, C. F. 1989, ApJ, 342, 306
- Houck, J., et al. 2004, ApJS, this volume.
- Lorenzetti, D., Tommasi, E., Giannini, T., et al. 1999, A&A, 346, 604
- Matthews, H. E., Purton, C. R., Roger, R. S., Dewdney, P. E., & Mitchell, G. F. 2003, ApJ, 592, 176
- McGroarty, F., Ray, T. P., & Bally, J. 2004, A&A, 415, 189
- Miskolczi, B., Tothill, N. F. H., Mitchell, G. F., & Matthews, H. E. 2001, ApJ, 560, 841
- Mitchell, G. F., & Matthews, H. E. 1994, ApJ, 423, 55
- Moro-Martín, A., Noriega-Crespo, A., Molinari, S., et al. 2001, ApJ, 555, 146
- Muzerolle, J., et al. 2004, ApJS, this volume.
- Racine, R. 1968, AJ, 72, 233
- Shevchenko, V. S., & Yakubov, S. D. 1989, Sov. Astron., 33, 370
- Strom, S. E., Strom, K. M., Yost, J., Carrasco, L., & Grasdalen, G. 1972 ApJ, 173, 353
- Timmerman, R., Bertoldi, F., Wright, C. F., et al. 1996, A&A, 315, L281
- Werner, M., et al. 2004a, ApJS, this volume
- Werner, M., Uchida, K., Selgren, K., et al. 2004b, ApJS, this volume
- Wilgenbus, D., Cabrit, S., Pineau des Forets, G., & Flower, D. R. 2000, A&A, 356, 1010
- Wright, C., Drapatz, S., Timmermann, R., van der Werf, P. P., Katterloher, R., & de Graauw, Th. 1996, A&A, 315, L301